nature materials

ARTICLES

PUBLISHED ONLINE: 8 MARCH 2009 | DOI: 10.1038/NMAT2403

A one-dimensional ice structure built from pentagons

Javier Carrasco[1,2], Angelos Michaelides[1,2]*, Matthew Forster[3], Sam Haq[3], Rasmita Raval[3] and Andrew Hodgson[3]

Heterogeneous ice nucleation has a key role in fields as diverse as atmospheric chemistry and biology. Ice nucleation on metal surfaces affords an opportunity to watch this process unfold at the molecular scale on a well-defined, planar interface. A common feature of structural models for such films is that they are built from hexagonal arrangements of molecules. Here we show, through a combination of scanning tunnelling microscopy, infrared spectroscopy and density-functional theory, that about 1-nm-wide ice chains that nucleate on Cu(110) are not built from hexagons, but instead are built from a face-sharing arrangement of water pentagons. The pentagon structure is favoured over others because it maximizes the water–metal bonding while maintaining a strong hydrogen-bonding network. It reveals an unanticipated structural adaptability of water–ice films, demonstrating that the presence of the substrate can be sufficient to favour non-hexagonal structural units.

In view of the familiarity and seeming simplicity of ice nucleation, our understanding of the molecular processes involved remains in its infancy, without any clear model for heterogeneous ice nucleation on the nanoscale. So far the clearest insight into the molecular details of the initial stages of ice nucleation has come by means of experimental and theoretical surface science techniques, which enable determination of how individual water molecules arrange on well-defined solid substrates[1–12]. Through such studies a tremendous array of water–ice structures, ranging from individual water hexamers to extended hexagonal one-dimensional (1D), 2D and 3D overlayers, have been reported. These studies have not been free from controversy, however, with numerous conflicts over the nature of the structures formed, most notably in recent years over the existence or otherwise of the standard hexagonal 'bilayer' model or whether some of the water molecules in the structures dissociate[3,4,7–16]. Nevertheless, a common feature of structural models discussed at present is that they are built from hexagonal arrangements of molecules.

Here, we investigate the initial stages of ice nucleation on a Cu(110) substrate. Water is found to aggregate into about 1-nm-wide chains, as previously reported[1,2]. However, we show, through a combination of scanning tunnelling microscopy (STM), reflection absorption infrared spectroscopy (RAIRS) and density-functional theory (DFT), that the ice chains are not built from hexagons, but instead are built from a face-sharing arrangement of water pentagons. Analysis of the atomic and electronic structures of the various overlayers considered, reveals that the pentagon structure is favoured over others (such as 1 and 2D hexagonal overlayers) because it maximizes the proportion of water molecules that interact strongly with the substrate while maintaining relatively strong hydrogen bonding with minimal strain within the overlayer. Calculations on other face-centred-cubic (f.c.c.) (110) surfaces suggest that the lattice constant of the substrate has the decisive role in the balance between pentagon and hexagon motifs.

Dosing water to sub-monolayer (ML) coverage resulted in the formation of ordered 1D chains, as previously reported[1,2] (Fig. 1). These chains are highly reproducible, forming across the entire temperature range explored (100–140 K), although they become labile at the lowest coverage (short chains) and at the higher temperatures. At low coverage (less than about 0.3 ML, estimated from both STM and RAIRS), water forms exclusively 1D chains at all temperatures examined. As the coverage is increased, the chains get closer to each other until this phase saturates with the chains still separated by at least 10 Å from each other. At higher coverage (greater than about 0.3 ML), regions of an extended 2D structure form, which coexist with the 1D chains. There is no evidence that 2D island formation is kinetically inhibited, for example, by a reduction in the chain density as 2D islands form, or that the chain density is sensitive to the temperature or water adsorption rate. RAIRS shows that 1D chains are reformed on heating high-coverage structures (such as the complete high-coverage 2D (7×8) structure[15] or multilayers) to desorb water and decrease the coverage, consistent with the observation of Yamada *et al.* of 1D chains being formed following desorption of water multilayers[1]. Although caution must in general be exercised in considering how kinetic aspects of ice film preparation can change the relative proportion of different phases observed, the evidence described strongly suggests that 1D chains are the thermodynamically stable phase for water on Cu(110) at low coverage.

The 1D chains are characterized by bright 'zigzagged' protrusions that run along the [001] direction, with a period of 7.2 Å. High-resolution images of the Cu surface show that the protrusions sit above the troughs between the Cu rows (Fig. 1c), consistent with the previous study[1]. Some images (Fig. 1b) partially resolve the structure within the chains, showing a depression adjacent to the bright protrusions, which suggests the chains consist of hydrogen-bonded rings of water linked along the [001] direction. The lateral separation of the bright protrusions is 5.4 ± 0.4 Å. This is smaller than previously reported—a fact that we attribute to the better resolution obtained here—and inconsistent with the earlier suggestion that these protrusions represent an entire water hexamer[1]. We note that although water adsorbs and desorbs intact on clean Cu(110) (refs 15, 16), partial dissociation stabilizes adsorption, forming a $c(2 \times 2)$ structure[17]. By a careful series of studies of different partially dissociated OH/H_2O structures formed by O/water co-adsorption, we established that the chains under consideration here consist exclusively of intact water molecules (see Supplementary Information for more details).

[1]Fritz-Haber-Institut der Max-Planck-Gesellschaft, Faradayweg 4-6, D-14195 Berlin, Germany, [2]Materials Simulation Laboratory, London Centre for Nanotechnology and Department of Chemistry, University College London, London WC1E 6BT, UK, [3]Surface Science Research Centre, The University of Liverpool, Liverpool L69 3BX, UK. *e-mail: angelos.michaelides@ucl.ac.uk.

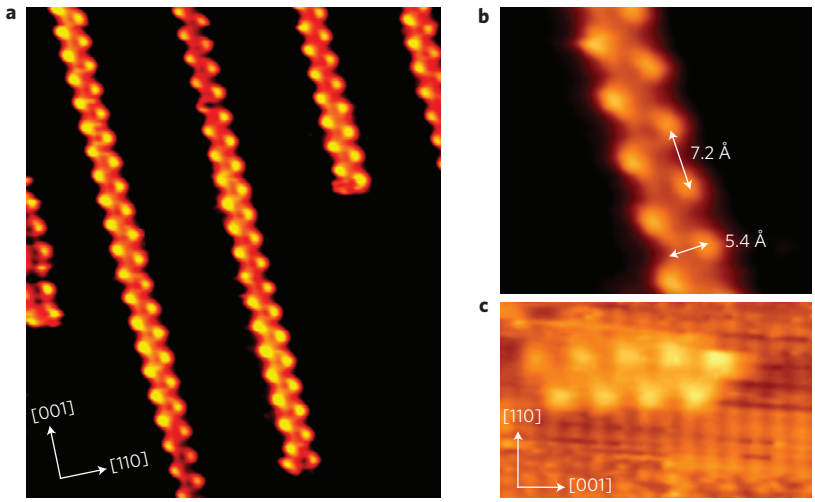

Figure 1 | Experimental STM images of water on Cu(110). a, STM image taken at 100 K showing water chains growing along the [001] direction (120 × 140 Å, $V = -196$ mV, $I = -0.63$ nA). **b**, Expansion of **a** showing partial resolution of the water structure within the chain (38 × 35 Å). **c**, Image showing protrusions residing between the Cu rows in the [001] direction (50 × 30 Å, $V = -196$ mV, $I = -0.34$ nA).

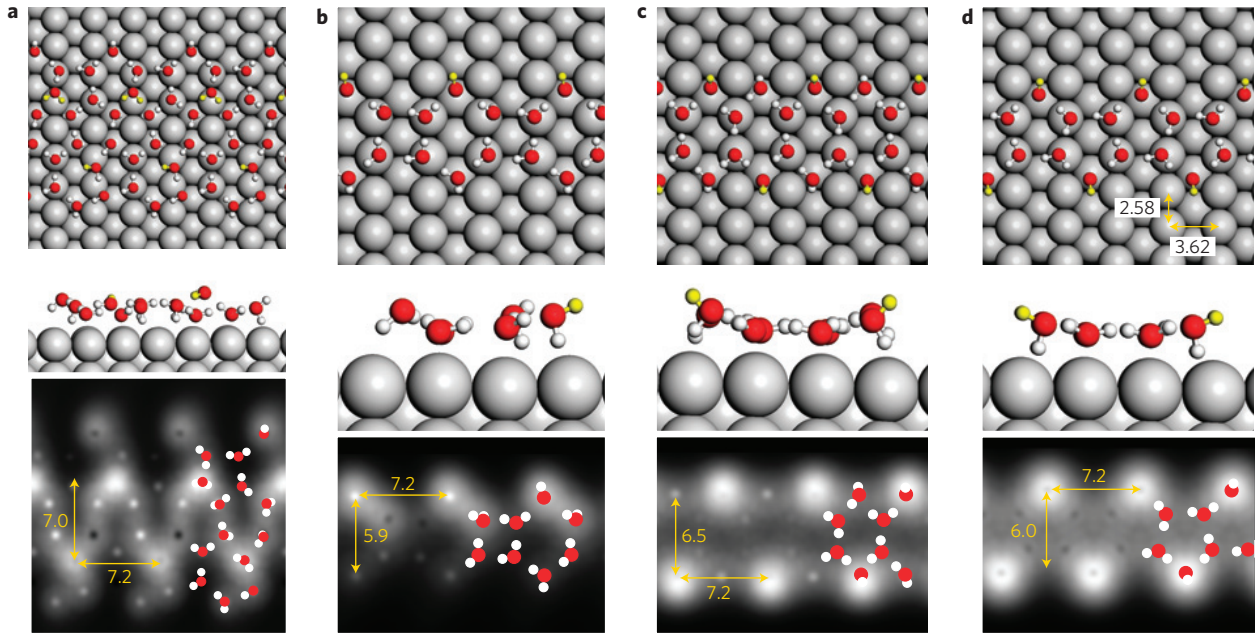

Figure 2 | Models for 1D water chains on Cu(110). a–d, Equilibrium geometry and simulated STM images for a selection of structures identified with DFT for water chains on Cu(110). Grey spheres correspond to Cu atoms, red ones to O atoms and small white ones to H atoms. The highest H atoms of each structure, which are responsible for the brightest features in the simulated STM images, are highlighted in yellow. In the simulated STM images, the locations of the water molecules in one surface unit are also shown. The most stable structure and the one we claim is observed in experiment is **d**, the pentagon-based structure. Distances are in Å.

Extended ice structures on metal surfaces are typically interpreted as being built from cyclic hexagons, related more or less to the hexagonal bilayer structure of the [0001] basal plane of ice I_h (ref. 18). This includes the ice structures that form on non-hexagonal metal surfaces, such as the (110) face of f.c.c. metals such as the Cu(110) substrate considered here[13–15]. On this basis, when applying DFT to calculate structural models of the chains, we first considered models based on hexagonal building blocks. All reported metal-supported ice-like models were considered, including the two hexamer-based structures suggested for this specific system (for example, those depicted in Fig. 2a,b)[1,5,6,10,19]. From these calculations, several minimum-energy structures were arrived at such as those shown in Fig. 2a–c, of which the adsorption energies, E_{ads}^{TOT}, are reported in Table 1. However, on simulating the STM images of the corresponding structures, it was clear that none was entirely satisfactory. In particular, the hexameric structure offering the most compelling agreement with the experimental STM images (Fig. 2c) was noticeably less stable (by 0.04 eV/H_2O) than a structure that offered very poor agreement with experiment (Fig. 2b), as well as having a similar stability to other non-zigzag structures.

From the simulated STM images it was clear that the bright features responsible for the main contrast in the images are likely to be the OH groups of individual water molecules, which 'dangle' away from the surface. We, therefore, considered structures consisting of H-bonded networks of water molecules with alternating arrangements of dangling OH groups and the initial assumption

Table 1 | DFT adsorption energies, E_{ads}^{TOT}, of 1D chains on Cu(110), along with estimates of the water–water, $E_{gas}^{H_2O-H_2O}$, and water–metal, $E_{ads}^{H_2O-Cu}$, bonding in these structures.

Model	E_{ads}^{TOT}	$E_{gas}^{H_2O-H_2O}$	$E_{ads}^{H_2O-Cu}$
Fig. 2a	0.54	0.33	0.21
Fig. 2b	0.56	0.29	0.27
Fig. 2c	0.52	0.23	0.29
Fig. 2d	0.59	0.29	0.30

The structure with the largest adsorption energy is one based on pentagons (Fig. 2d). The units are eV/H_2O.

that the overlayer should be built exclusively from hexamers was dropped. This extended DFT-based structural search consisted of an extensive set of structures built from arrangements of hexamers, pentamers and tetramers, and combinations thereof. The lowest energy structure identified in this search and, indeed, the lowest energy of any water chain structure is one consisting of a face-sharing arrangement of water pentagons (Fig. 2d). Note that this conclusion is unaltered when other DFT exchange–correlation functionals are considered or contributions such as zero-point energies or finite-temperature vibrational free-energy effects are accounted for (see Supplementary Information for more details). Furthermore, the simulated STM image of the pentagon structure offers good agreement with experiment, reproducing the characteristic zigzag pattern with the correct periodicity along the [001] plane (7.2 Å between bright features), approximately correct width (6.0 Å) and with the bright features correctly located over the troughs of the (110) surface.

RAIRS of the 1D chains offers further support for the claim that they are built from pentagons (Fig. 3a). The water chains have a distinct vibrational spectrum, quite different from that of the 2D ice monolayer that forms on this surface at saturation[15]. Specifically, RAIRS finds sharp, intense vibrational bands at 3,627, 3,197, 1,573 and 753 cm^{-1}, along with broader less intense features near 3,440, 3,300 and 1,620 cm^{-1} (Fig. 3a). On calculation of the infrared spectrum of the pentagon and certain hexagon structures, we find the best agreement is again offered by the pentagon structure. Indeed, in the computed infrared spectrum of the pentagon structure (Fig. 3d), all of the experimental vibrations are present at approximately the correct frequency with approximately correct relative intensities. In particular, the intense free O–H stretches are at 3,696 and 3,163 cm^{-1} compared to the experimental values of 3,627 and 3,197 cm^{-1}, whereas alternative structures exhibit a much greater range of frequencies (Fig. 3b,c), as well as more (and higher frequency) librational bands than are observed (Fig. 3a). In addition, two molecular scissors bands are observed in experiment, a sharp low-frequency band at 1,573 cm^{-1} and the hydrogen-bonded scissors near 1,620 cm^{-1}. Calculations for the pentamer chain reproduce the correct number of bands, with a hydrogen-bonded scissors band near 1,615 cm^{-1} and a sharp band at 1,545 cm^{-1} associated with the molecules located over the troughs in the pentagon structure, which are not involved in donating any hydrogen bonds. In contrast, calculations for the other structures (Fig. 3b,c) show two sharp scissors bands at or below 1,600 cm^{-1}, in addition to the weak hydrogen-bonded water band, and are inconsistent with experiment. Inspection of the computed eigenmodes reveals that across the entire spectrum the intense stretching bands are associated with the non-donor water molecules located above the Cu(110) trenches.

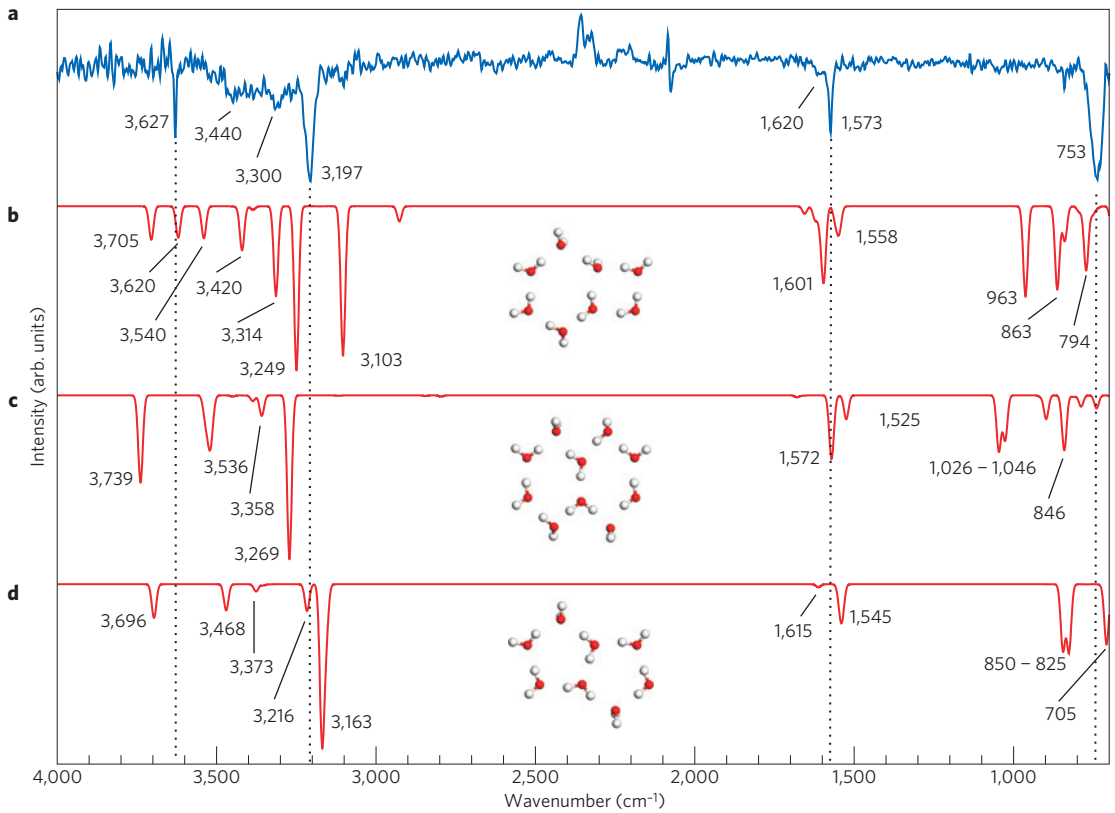

Figure 3 | Experimental and computed infrared spectra for 1D water chains on Cu(110). a, Experimental RAIRS spectrum for water chains (about 0.3 θ_{sat}) at 146 K. **b**,**c**, Computed infrared spectra for the hexagon-based structures shown in Fig. 2b and c, respectively. **d**, Computed infrared spectrum for the pentagon-based 1D chains shown in Fig. 2d.

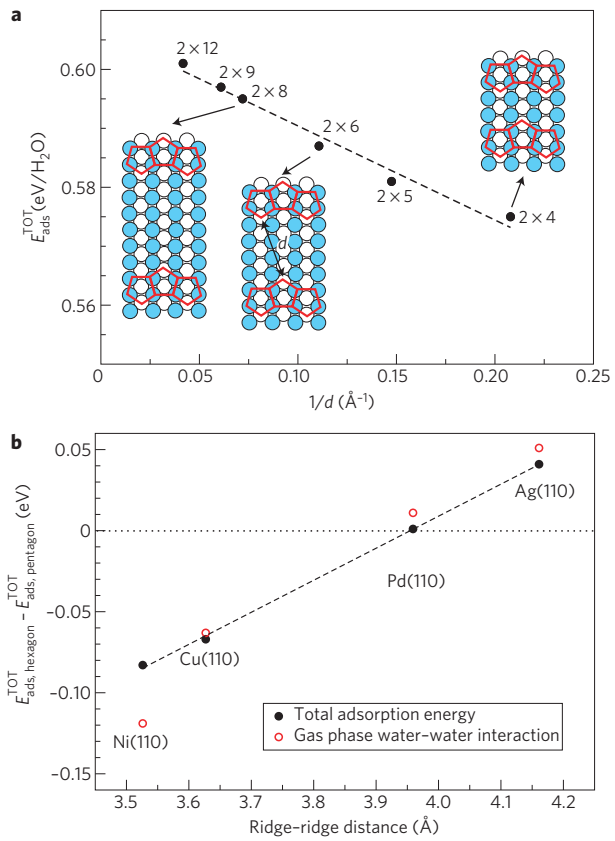

Figure 4 | Interaction between pentagon chains and relative energies of hexagon and pentagon chains on various metal surfaces. a, Adsorption energies of pentagon chains versus $1/d$, where d is the shortest distance between atoms in adjacent chains. The labels for each point stand for the supercell used in the simulation. **b**, Adsorption energy difference between hexagon- (Fig. 2c type) and pentagon-based (Fig. 2d type) 1D chains as a function of the metal substrate. Negative values denote a preference for pentagonal chains. The differences in the gas-phase water–water interaction within each overlayer structure are also reported.

Finally, the pentagon model is consistent with the observation from STM that chains maximize their separation from each other and transform into a 2D overlayer structure at high coverage. Specifically, DFT calculations of the interaction between chains—carried out by using unit cells with different widths—find a continuous drop in adsorption energy (destabilization) as the separation, d, between chains is reduced (Fig. 4a). This interaction follows a linear $1/d$ dependence, characteristic of electrostatic (charge–charge) repulsion, the chains repelling each other and becoming increasingly unstable as they are forced closer together with increasing coverage. The $1/d$ dependence suggests that the repulsion is dominated by through-vacuum repulsion and that the image charge in the metal does not have a significant influence on the form of the repulsion. At some point the stability of the 1D chains drops below that of the 2D overlayer, at which point the 2D phase will nucleate. Experimentally this is seen to occur only once chains are forced within about 10–15 Å of each other during growth, causing water to abandon the commensurate adsorption site to form the complex 2D (7×8) structure[15].

We now consider why a 1D pentagon chain structure forms on this surface. Two factors are important. First there is the interaction with the substrate. This is strongest for flat-lying water molecules at atop sites of the Cu ridges. All low-energy structures identified have a large proportion of water molecules at these sites, pinning the overlayer into registry with the substrate. The pentagon structure is particularly favourable with two thirds of the water molecules on Cu ridges and consequently the strongest water–metal interaction of the overlayers considered (Table 1). Second there is the water–water (hydrogen bonding) interaction. Here, we find that the optimal hydrogen-bonding arrangement is not necessarily the one with the largest proportion of hydrogen bonds per water molecule—as a traditional hexagonal 2D bilayer would have—but rather the one that achieves the strongest hydrogen bonds with minimal strain within the overlayer. Indeed, fitting commensurate arrangements of hexagons across the [110] rows of the Cu substrate—as chains (for example, Fig. 2c) or the (unrepresentatively) high-symmetry 2D overlayer reported in refs 13, 14—requires about 1 Å compression of each hexagon compared with the ideal hexagonal geometry of ice. This introduces strain in the overlayers, which thus destabilizes these structures; for example, the commensurate hexagon-based 1D chain (Fig. 2c) has an adsorption energy of 0.52 eV/H_2O and the $c(2 \times 2)$ water structure reported in[13,14] an adsorption energy of 0.54 eV/H_2O, within the current computational set-up. In contrast, the staggered arrangement of smaller pentagons, with an adsorption energy of 0.59 eV/H_2O, makes a better fit to the substrate. The idea that the strength of the hydrogen bonding within the overlayer is important to the relative stability of the structures formed can be tested by calculations of the various 1D structures in the gas phase (that is, without the substrate). These calculations find that, fixed in the structures they assume on adsorption, a gas-phase 1D chain of pentagons is 0.06 eV/H_2O more stable than a chain of hexagons. This matches almost exactly the 0.07 eV/H_2O preference for pentagons over hexagons on the surface. Extensive tests with other DFT exchange–correlation functionals and with Møller–Plesset perturbation theory on the relative stability of the relevant pentamer and hexamer motifs in the gas phase demonstrate that the conclusion on relative stabilities arrived at here is not sensitive to our particular choice of exchange–correlation functional (see Supplementary Information for more details). Formation of the 2D structure at higher coverage presumably alleviates strain by abandoning the simple commensurate adsorption site and adopting a (7×8) periodicity. Exploring the details of this phase transition with DFT requires characterization of the complex 2D (7×8) structure, about which little is known[15].

Let us now place the present results in a broader context and consider how ice might nucleate on other f.c.c. (110) surfaces. To this end, DFT was used to determine the structure and relative stability of 1D chains of hexagons and pentagons on the (110) surfaces of Ni, Pd and Ag. Along with Cu, this consists of a set of four (110) substrates with a separation between the close-packed [110] ridges that ranges from about 3.5 Å to about 4.2 Å. As shown in Fig. 4b, an interesting correlation between the relative stability of hexagon versus pentagon chains is observed. Pentagons are favoured on substrates with small lattice constants; that is, in addition to Cu, Ni is identified as a substrate on which pentagons may nucleate. Pd is a borderline case, whereas on the substrate with the largest lattice constant Ag, there is a small preference for hexagons. The trend in the relative stability of hexamers versus pentamers as a function of lattice parameter also holds for these structures in the gas phase (open circles in Fig. 4b), providing extra support that hydrogen bonding within the water layers is key to the relative stability of hexamer versus pentamer chains.

In summary, a combination of experimental scanning probe techniques, infrared vibrational spectroscopy and DFT leads to the characterization of an ice-like structure built from pentagon units. Although there is a precedent for pentagon-based ice structures in other environments[20,21], this is the first time that such a structural unit has been seen at a surface. The nucleation of pentagons reveals an unanticipated adaptability of water–ice films to optimize bonding within the overlayer and to the surface. In general, the detailed arrangement of water at interfaces is

not known from experiment and future studies should focus on identifying structures that optimize the balance between water–metal and water–water bonding, rather than concentrating overly on hexagonal packing arrangements.

Methods

Experimental. Images of water adsorbed on Cu(110) were recorded at 100 K in an ultrahigh vacuum STM (Specs 150) operated in constant-current mode with an electrochemically etched tungsten tip. The Cu surface was prepared by argon ion sputtering at 500 eV followed by annealing to 800 K and showed an average terrace size of about 800 Å. Ultrapure (10^7 Ω cm) water was dosed from background gas at a pressure of 2×10^{-9} mbar. To ensure the chain structure observed is not caused by tip-induced re-structuring, images were taken using a variety of scanning angles and tunnelling conditions; all images yielded an identical structure oriented along [001], thus showing the negligible effect of the tip on the corresponding water structure. Reflection absorption infrared spectra were recorded at 80 K by a Mattson 6020 Fourier-transform infrared spectrometer, operated at the glancing angle with 4 cm^{-1} resolution using a broadband mercury cadmium telluride detector (650–4,000 cm^{-1}) to record the OH stretching and libration regions simultaneously. The water coverage is estimated by calibrating the water dose against that required to form a complete monolayer (θ_{sat}) as determined by temperature-programmed desorption.

Theoretical. The calculations involve DFT and supercell periodic models as implemented in the Vienna Ab-initio Simulation Package code[22,23]. The Perdew–Burke–Ernzerhof[24] exchange–correlation functional has been used and the inner electrons replaced by projector augmented wave pseudopotentials[25], expanded in a basis set of plane waves up to a cutoff energy of 415 eV. A Monkhorst–Pack grid with at least $12 \times 12 \times 1$ **k**-point sampling per 1×1 cell was used. Water/Cu(110) structures were modelled in p($2 \times n$) unit cells, with n from 3 to 12. In all cases reported, a four-layer Cu slab was used separated by a 14 Å vacuum. The two bottom layers have been fixed to their bulk Perdew–Burke–Ernzerhof-optimal positions ($a_{Cu} = 3.627$ Å) during structure optimization procedures, with all other atoms fully relaxed. All of the above choices of computational set-up have been carefully checked through an extensive series of test calculations, some of which are reported in Supplementary Information. STM images were simulated with the Tersoff–Hamann approach[26], with a voltage of −200 meV and at a height of 6 Å above the metal surface. Vibrational frequencies were determined with a standard finite displacement method; the infrared intensities were calculated by estimating numerically the z component of the dipole moment derivative with respect to displacements along the z Cartesian component (see Supplementary Information for details).

Adsorption energies, E_{ads}^{TOT}, per water molecule are obtained by subtracting the energy of the adsorbed $n$$H_2O$ adstructure from the sum of the energies of the relaxed bare metal slab and n isolated gas phase H_2O molecules. The estimate of the water–water bonding, $E_{gas}^{H_2O-H_2O}$, is simply the water–water bonding in the gas-phase water structure in the absence of the substrate, but with all atoms fixed in the precise geometries they adopt in the adsorption structure[27]. The estimate of the water–Cu bonding, $E_{ads}^{H_2O-Cu}$, is simply taken as the difference between E_{ads}^{TOT} and $E_{gas}^{H_2O-H_2O}$.

Received 18 July 2008; accepted 9 February 2009; published online 8 March 2009

References

1. Yamada, T., Tamamori, S. & Okuyama, H. Anisotropic water chain growth on Cu(110) observed with scanning tunneling microscopy. *Phys. Rev. Lett.* **96**, 036105 (2006).
2. Lee, J., Sorescu, D. C., Jordan, K. D. & Yates, J. T. Jr. Hydroxyl chain formation on the Cu(110) surface: Watching water dissociation. *J. Phys. Chem. C* **112**, 17672–17677 (2008).
3. Feibelman, P. J. Partial dissociation of water on Ru(0001). *Science* **295**, 99–102 (2002).
4. Menzel, D. Surface science—Water on a metal surface. *Science* **295**, 58–59 (2002).
5. Michaelides, A. & Morgenstern, K. Ice nanoclusters at hydrophobic metal surfaces. *Nature Mater.* **6**, 597–601 (2007).
6. Cerda, J. *et al.* Novel water overlayer growth on Pd(111) characterized with scanning tunneling microscopy and density functional theory. *Phys. Rev. Lett.* **93**, 116101 (2004).
7. Ogasawara, H. *et al.* Structure and bonding of water on Pt(111). *Phys. Rev. Lett.* **89**, 276102 (2002).
8. Andersson, K., Nikitin, A., Pettersson, L. G. M., Nilsson, A. & Ogasawara, H. Water dissociation on Ru(001): An activated process. *Phys. Rev. Lett.* **93**, 196101 (2004).
9. Weissenrieder, J., Mikkelsen, A., Andersen, J. N., Feibelman, P. J. & Held, G. Experimental evidence for a partially dissociated water bilayer on Ru(0001). *Phys. Rev. Lett.* **93**, 196102 (2004).
10. Haq, S., Clay, C., Darling, G. R., Zimbitas, G. & Hodgson, A. Growth of intact water ice on Ru(0001) between 140 and 160 K: Experiment and density-functional theory calculations. *Phys. Rev. B* **73**, 115414 (2006).
11. Meng, S., Wang, E. G. & Gao, S. W. Water adsorption on metal surfaces: A general picture from density functional theory studies. *Phys. Rev. B* **69**, 195404 (2004).
12. Yang, Y., Meng, S. & Wang, E. G. Water adsorption on a NaCl (001) surface: A density functional theory study. *Phys. Rev. B* **74**, 245409 (2006).
13. Ren, J. & Meng, S. Atomic structure and bonding of water overlayer on Cu(110): The borderline for intact and dissociative adsorption. *J. Am. Chem. Soc.* **128**, 9282–9283 (2006).
14. Ren, J. & Meng, S. First-principles study of water on copper and noble metal (110) surfaces. *Phys. Rev. B* **77**, 054110 (2008).
15. Schiros, T. *et al.* Structure of water adsorbed on the open Cu(110) surface: H-up, H-down, or both? *Chem. Phys. Lett.* **429**, 415–419 (2006).
16. Andersson, K. *et al.* Molecularly intact and dissociative adsorption of water on clean Cu(110): A comparison with the water/Ru(001) system. *Surf. Sci.* **585**, L183–L189 (2005).
17. Bange, K., Grider, D. E., Madey, T. E. & Sass, J. K. The surface-chemistry of H_2O on clean and oxygen-covered Cu(110). *Surf. Sci.* **136**, 38–64 (1984).
18. Thiel, P. A. & Madey, T. E. The interaction of water with solid-surfaces—fundamental-aspects. *Surf. Sci. Rep.* **7**, 211–385 (1987).
19. Schiros, T. *Water-Metal Surfaces*. Doctoral Thesis in Chemical Physics (Stockholm Univ. 2008).
20. Ma, B.-Q., Sun, H.-L. & Gao, S. Cyclic water pentamer in a tape-like structure. *Chem. Commun.* 2220–2221 (2004).
21. Naskar, J. P., Drew, M. G. B., Hulme, A., Tocher, D. A. & Datta, D. Occurrence of ribbons of cyclic water pentamers in a metallo-organic framework formed by spontaneous fixation of CO_2. *Cryst. Eng. Comm.* **7**, 67–70 (2005).
22. Kresse, G. & Hafner, J. Ab initio molecular-dynamics for liquid-metals. *Phys. Rev. B* **47**, 558–561 (1993).
23. Kresse, G. & Furthmüller, J. Efficient iterative schemes for ab initio total-energy calculations using a plane-wave basis set. *Phys. Rev. B* **54**, 11169–11186 (1996).
24. Perdew, J. P., Burke, K. & Ernzerhof, M. Generalized gradient approximation made simple. *Phys. Rev. Lett.* **77**, 3865–3868 (1996).
25. Kresse, G. & Joubert, D. From ultrasoft pseudopotentials to the projector augmented-wave method. *Phys. Rev. B* **59**, 1758–1775 (1999).
26. Tersoff, J. & Hamann, D. R. Theory and application for the scanning tunneling microscope. *Phys. Rev. Lett.* **50**, 1998–2001 (1983).
27. Michaelides, A., Alavi, A. & King, D. A. Insight into H_2O-ice adsorption and dissociation on metal surfaces from first-principles simulations. *Phys. Rev. B* **69**, 113404 (2004).

Acknowledgements

J.C. acknowledges financial support from the Alexander von Humboldt Foundation and the Royal Society. A.M.'s work is supported by a EURYI award (see www.esf.org/euryi) and by the EPSRC. A.H. acknowledges support by the EPSRC and R.R. by the EPSRC and BBSRC. Through our membership of the UK's HPC Materials Chemistry Consortium, which is funded by the EPSRC (EP/F067496), this work made use of the facilities of HECToR, the UK's national high-performance computing service, which is provided by UoE HPCx Ltd at the University of Edinburgh, Cray Inc and NAG Ltd, and funded by the Office of Science and Technology through EPSRC's High End Computing Programme. We are also grateful to the London Centre for Nanotechnology for computational resources and to Peter Feibelman for his helpful comments on an earlier version of this manuscript.

Additional information

Supplementary information accompanies this paper on www.nature.com/naturematerials. Reprints and permissions information is available online at http://npg.nature.com/reprintsandpermissions. Correspondence and requests for materials should be addressed to A.M.